Int J Adv Manuf Technol (2015) 78:907–915
DOI 10.1007/s00170-014-6699-1

ORIGINAL ARTICLE

A novel Bi-processing technique for metal matrix nanocomposites

Ashraf A. Ali · M. A. H. El-Meniawi · S. M. Khafagi

Received: 14 September 2014 / Accepted: 9 December 2014 / Published online: 20 December 2014
© Springer-Verlag London 2014

Abstract The main problem of reinforcing metal matrix with nanoreinforcements is how can each single nanoreinforcement be well dispersed or/and aligned in a specific location and direction without any agglomeration or randomness. This study presents a novel solid-state Bi-processing technique for forming homogenous metal matrix nanocomposites (MMNCs). In this paper, carbon nanotubes (CNTs) of three weight concentrations were dispersed in precursor carbon polymer solution (PCPS). CNTs/PCPS dispersions were electrospun under optimum electrospinning conditions, and the collected hybrid CNT/precursor carbon nanofibril (CNF) hybrid fabrics were thermally stabilized under a static pressure in two steps to activate its high surface energy aiming to build strong and flexible CNT/CNF hybrid fabrics of 60-MPa strength. The flexible hybrid CNT/CNF fabrics were then placed in fine grooves that were machined in pure aluminum metal substrate. Then, friction stir process (FSP) was applied to produce aligned and well-dispersed CNT/CNF hybrid fabrics in aluminum matrix. Morphological characterization by using scanning electron microscope (SEM) and high-resolution transmission electron microscope (HRTEM) were conducted. Also, tensile and micro-hardness properties were evaluated in detail. The results proved the possibility of producing MMNCs by using Bi-processing technique (electrospinning and FSP) for the first time in literature.

A. A. Ali (✉)
Mechanical Design and Production Engineering Department, Faculty of Engineering, Zagazig University, P.O. Box 44519, Markaz El-Zakazik, Egypt
e-mail: ashali@zu.edu.eg

M. A. H. El-Meniawi
Materials Engineering Department, Faculty of Engineering, Zagazig University, Markaz El-Zakazik, Egypt

S. M. Khafagi
Tabbin Institute for Metallurgical Studies (TIMS), Helwan, Egypt

Keywords Electrospinning · FSP · MMNCs · SEM · HRTEM · Mechanical properties

1 Introduction

Optimization of electrospinning process to produce minimum polymer fiber diameters have been studied for more than a decade. Most of these publications [1–6] were focusing on specified processing parameters such as Berry's number, charge density, spinning angle, spinneret diameter, and spinning distance as the most influencing processing parameters on the electrospun nanofiber diameters. Electrospun nanofibers are characterized by its high surface area; this characterization showed a different behavior for the nanosized fibers such as super absorbent characteristics for electrospun polyacrylamide (PAM) nanofibers. Fourfold increase in absorbent capacity has been reported for the processed PAM nanofibers more than original microsized particulate one [7]. Nanoreinforcement size effect has been reported for carbon nanotube-reinforced carbon nanofibers. Also, it has been proved that fibril composites in nanolevel do not obey tradition physics and mechanics such as rule of mixture and Hooke's law [8]. Also, the effect of graphite nanoplatelets as reinforcement nanomaterials with carbon nanofibers has showed a nanosize effect on the rule of mixture [9]. In these previous two papers [8, 9], nanoreinforcement effect has been correlated to the unusual behavior of molecular chains (free atoms) on the surface of nanoscale fibers.

It is well known that atoms at a free surface experience a different local environment than do atoms in the bulk of a material; as a result, the energy associated with these atoms will, in general, be different from that of the atoms in the bulk. The excess energy associated with surface atoms is called surface-free energy. In traditional continuum mechanics, such surface-free energy is typically neglected because it is

associated with only a few layers of atoms near the surface and the ratio of the volume occupied by the surface atoms and the total volume of material of interest is extremely small. However, for nanosize materials such as nanofibers, the surface-to-volume ratio becomes significant and so does the effect of surface free energy [10].

The effect of surface energy on the elastic behavior at the nanolevel has been studied in literature. For example, Dingreville et al. [11] showed 20 % increase in the axial Young's modulus for 4-nm-diameter copper wire. Also, Nanda et al. [12] showed 5–6 times increase in material surface energy for Ag nanoparticles relative to bulk.

One important discovery by He et al. [13] is a size effect in the elastic property of electrospun PAN nanofibers only below 150 nm that has been found. On the other hand, nanodiamond nucleation has been reported for carbon nanomaterials below the required pressure and temperature for similar bulk materials [14]. Sun et al. [15] showed a formation of nanodiamond from carbon nanotube wires. In general, the last two papers [14, 15] proved that materials in nanolevel behave thermodynamically different than do materials in bulk.

Ali and co-workers [10, 16, 17] start to utilize the high surface energy associated with the electrospun PAN nanofibers along with different nanoreinforcements such as carbon nanotube and copper nanoparticles and use it as a cohesive bond aiming to build a firm, strong, and flexible precursor carbon nanofibril hybrid fabrics and also to utilize the high degree of entanglement inside the electrospun nanofibril composite structures to gain a higher degree of flexibility for such hybrid fabrics.

Based on the previous literature, it can be concluded that electrospinning is a unique and simple process which can be used to produce polymer matrix nanocomposites (PMNCs) and carbon-carbon nanocomposites (CCNCs) with different types of well-dispersed and aligned nanoreinforcements as well as well-controlled weight percentages. On the other hand and unfortunately, electrospinning is not suitable as a process alone and by itself to produce metal matrix nanocomposites (MMNCs).

In recent years, aluminum metal matrix composites (AMMCs) have been used in the aerospace, aircraft, and automotive industries, particularly for lightweight cylinder liners because AMMCs have many advantages, including higher strength, higher wear resistance, higher thermal conductivity, and lower coefficient of friction.

A proper technique can be employed to refine the microstructure and homogeneous disperse of reinforcements on metallic surface ever since wear is surface deprivation property [18]. Dispersion of reinforcement particles on metal surface and the control of its dispersal are more difficult to attain by conventional surface modification techniques. Previous researchers [19, 20] reported that thermal spraying and laser beam techniques were utilized to prepare surface composites, in which it degrades the properties due to formation of unfavorable phases. These techniques are operated at higher temperatures and impossible to avoid the reaction between the reinforcements and the matrix, which forms detrimental phase. A process can be employed which is operated at below melting temperature of matrix for the fabrication of surface composites which can avoid the abovementioned complications. Considering the above problems, friction stir process (FSP) is best suited for the preparation of surface composites and surface modification. In FSP, a rotating tool with shoulder and pin is plunged into the surface of material, which creates frictional heat and dynamic mixing of material area underneath of the tool [21]. It leads to incorporate and/or disperse the reinforcement particles in the matrix material such as aluminum alloys, magnesium alloys, and copper [22–24]. The authors [25] have achieved in homogeneous dispersion of SiC particles (20-μm average size) on a surface of aluminum alloy 6061-T6 via FSP. Hybrid composites are prepared by reinforcing with a mixture of two or more different types of particles which combines the individual properties of each type of particle.

Recently, much attention has been paid to the friction stir processing (FSP) for its promise as a solid-state surface modification technique [26–28]. A rotating tool with a specially designed pin and shoulder is inserted into a substrate and produces a highly plastically deformed zone (stir zone). It is well known that the stir zone consists of fine and equiaxed grains produced by dynamic recrystallization. FSP has also been used to fabricate surface composites [29].

The FSP provides the following advantages: (1) a solid-state process to prevent problems associated with liquid metallurgy, (2) severe plastic deformation to promote mixing and refining of constituent phases in the material, and (3) hot consolidation to form fully dense solid. The basic concept of FSP is remarkably simple. A rotating tool with pin and shoulder is inserted in a single piece of material for microstructural modification and traversed along the desired line to cover the region of interest. Friction between the tool and work pieces results in localized heating that softens and plasticizes the work piece. A volume of processed material is produced by movement of materials from the front of the pin to the back of the pin [30]. During this process, the material undergoes intense plastic deformation, which results in significant grain refinement [31]. The optimum conditions of the rotational speed, transverse speed, tool penetration depth, and pin profile were found to be 1600 r/min, 40 mm/min, 0.30 mm, and threaded type, respectively [32].

Dispersion of the nano-reinforcements in a uniform manner is a critical and difficult task. It should be pointed out that the existing processing techniques for forming surface composites are based on liquid-phase processing at high temperatures. In this case, it is hard to avoid the interfacial reaction between reinforcement and metal matrix and the formation of some

detrimental phases. Furthermore, critical control of processing parameters is necessary to obtain ideal solidified microstructure in surface layer. Obviously, if processing of surface composite is carried out at temperatures below the melting point of substrate, these problems can be avoided. Recently, a lot of attention has been paid to FSP as a new surface modification technique. Though FSP has been basically advanced as a grain refinement technique, it can be readily used for fabricating surface composites. FSP induces intense plastic deformation and mixing of material in the processed zone [33].

In this paper, a novel idea of producing metal matrix nanocomposites (MMNCs) has been verified by using both electrospinning and FSP techniques. First, carbon nanotubes (CNTs) have been dispersed and aligned in PAN nanofibril composite fabrics by using electrospinning technique, and then the whole fabrics were heat-treated under static pressing technique to produce well-aligned, flexible, and strong CNT/carbon nanofibril (CNF) composite fabrics. Second, the produced CNT/CNF fabrics were placed in between two aluminum metal plates and FSP was applied to produce CNT/CNF/Al metal matrix nanocomposites as a final product at the desired weight percentage and alignment direction of CNTs that has been well controlled in the first processing step.

2 Experimental work

2.1 Electrospinning

CNTs of outside diameter=40–60 nm, inside diameter=5–10 nm, and length=0.5–500 μm were dispersed in dimethylformamide (DMF) by using SONOREX Digital 10P Bandel-model Sonicator for 24 h to ensure well dispersion of CNTs with three different concentrations 1, 3, and 5 wt.%; then, polyacrylonitrile (PAN) of 150,000 g/mol molecular weight from Aldrich was used with 10 wt.% concentration with DMF to form well-dispersed CNTs in precursor carbon polymer solution (PCPS/CNTs) after hot stirring for 3 h at 60 °C to ensure a complete PAN solubility in DMF and to form (PCPS/CNTs) 3 wt.% dispersions.

PCPS/CNTs dispersions were poured to fill a clean syringe of 10-ml volume, and the syringe was placed in a controlled pump set to give a flow rate of 0.025 ml/min. The syringe was connected to a rubber tube of 30-cm length and 2-mm inner diameter, and the other side of the rubber tube was connected to a metal tube of 35-cm length and 1.016-mm inner diameters. The metal tube was placed in a hole drilled in a circular aluminum disc of 15-cm diameter and 1-cm thickness; the aluminum disc was connected to the power supply at approximately 35 kV of positive potential. A metal screen collector of 15×15 cm dimensions was centered vertically at a 30-cm distance away from the orifice of the metal tube and was covered with aluminum foil. The potential was applied first; then, the pump flow rate was increased to ensure no droplet's accumulation on the metal screen collector which was covered with aluminum foil. The electrospun fibers were collected for about 8 h. Optimization of electrospinning processing conditions for minimum PAN nanofiber diameters and distribution have been presented and discussed in Ali's and co-workers previous work [10, 17, 34]. Also, live photo of the used electrospinning setup in the present work is shown in Fig. 1.

2.2 Hot-pressing

About 2 cm from each side of the collected fiber mat was trimmed; then, the mat was placed in between two aluminum plates of 110×105 mm dimensions and 10-mm thickness after it was covered with aluminum foil. The mold with the mat in between was placed in a hot press Carver, USA, model of maximum 10 metric tons and 500 °C, set to 220 °C with no applying pressure for 1 h until the plate's temperature reached the maximum set temperature. Then, 1 metric ton was applied for another 1 h. The hot press was then allowed to cool down for another 1 h while keeping the pressure on until it reaches 100 °C; then, the pressure was released completely from the fabric except the weight of the upper aluminum plate until it cooled down to room temperature [10, 34].

2.3 Friction stir process

Commercially available pure aluminum sheet with a dimension of 100×60×4 mm was used as base metal (BM). Three types of specimens were used for the FSP experiments (1, 3, and 5 wt.% CNT/CNF hybrid fabrics) in aluminum substrate.

The FSP tool was made of H13 steel having screwed taper pin profile with shoulder diameter of 16 mm and pin diameter of 4.5 mm, and 2.7-mm height was used. The CNTs/CNFs

Fig. 1 Electrospinning setup

hybrid fabrics at selected ratios were packed in the groove. The groove opening is initially closed by means of the tool which is having shoulder without pin to avoid the escapement of any of the fabrics from groove while processing. In all FSP experiments, tool rotation rate, traverse speed, and tilt of the spindle towards trailing direction were kept constant in this study to be 1040 rpm, 52 mm/min, and 2°, respectively.

2.4 Characterizations

2.4.1 Morphological characterizations

Structural characteristics of nanofibers after hot pressing as well as MMNCs after FSP have been investigated using scanning electron microscope (SEM) and high-resolution transmission electron microscope (HRTEM).

CNTs/carbon nanofibril composite fabrics characterizations Scanning electron microscope (SEM) model (JEOL JSM-5600LV) has been conducted for all CNT/CNF hybrid fabrics after being gold-coated. Also, HRTEM model (JEOL-JEM 2100) has been used to characterize the 3 wt.% CNT/CNF hybrid fabrics in details.

FSP samples After FSP, microstructural observations were carried out at the cross-section of nugget zone (NZ) or stirred zone (SZ) of CNTs/CNFs/Al MMNCs normal to the FSP direction, mechanically polished and etched with Keller's reagent (2 ml HF, 3 ml HCl, 20 ml HNO3, and 175 ml H2O) by employing optical microscope. Microstructures of the hybrid composites were captured and presented. The SEM is also utilized for measuring the reinforcement NZ and worn morphology of MMNCs.

2.4.2 Tensile testing

CNTs/carbon nanofibril composite fabrics testing Five tensile samples of 60-mm length and 5-mm width were cut from the hot-pressed nanofibril hybrid fabrics. Each sample has been weighted to an accuracy of three digits. A Zwick/Roell Z-100 model UTM with 500 N load cell and 1 μN accuracy has been used to investigate the tensile properties of the hot-pressed CNT/CNF hybrid fabrics [10, 17, 34].

FSP samples Five specimens from each CNT weight percent of (CNTs/CNFs/Al) MMNCs were taken normal to the FSP direction and made as per ASTM: E8/E8M-11 standard by using wire cut electrical discharge machining to the required dimensions. The tensile test is carried out on a computer-controlled UTM model (Zwick/Roell Z-100) at a cross head speed of 10 mm/min.

2.4.3 Micro-hardness testing

Micro-hardness tests were carried out at the cross-section of NZ of CNTs/CNFs/Al MMNCs normal to the FSP direction, samples with a load of 50 g and duration of 15 s using a Vickers digital micro-hardness tester model (LECO-LM 700).

3 Results and discussion

3.1 Morphological characterizations

Figure 2 shows a scanning electron microscope for the hot-pressed CNT/CNF hybrid fabrics for all three samples at different CNT weight percent. From Fig. 2, it can be noticed that the presence of CNTs reduces the diameter of nanofibril composites as it has been measured precisely in previous work ref. [34]. Also, it has no obvious effect on the fibril surface morphology, fibril distribution, or bead formation.

As shown in Fig. 3, high-resolution transmission electron microscopes have been conducted to 3 wt.% CNT/CNF hybrid fabrics. The figure proves the presence of CNTs inside the carbon nanofibers as shown in Fig. 3a, b. Also, separation of CNTs from CNFs (as shown in Fig. 3c requires, only, a 1-min stirring for CNTs/CNFs in DMF sample just to overcome the secondary physical bond between CNTs and CNFs which is much smaller than the induced force from FSP. From Fig. 3d, grapheme layers of 0.333 nm can be observed which proves a well-ordered and crystalline structure and explain the outstanding mechanical properties of single CNTs or/and single CNTs/CNFs as it has been reported by using AFM in previous work [34].

Figure 4 shows assembling of 34 consecutive SEM micrographs across the friction-stirred CNT/CNF/Al MMNC samples. The figure shows the distribution of CNT/CNF hybrid fabrics in aluminum substrate after FSP has been applied. The figure proves the perfect integration and well distribution between reinforcement and matrix forming CNTs/CNFs/Al MMNCs.

From Fig. 4, the area of CNTs/CNFs in SZ can be calculated to get the number of CNTs approximately as follows:

The NZ area is approximately 12 mm^2 or about (0.72 cm^3), assuming CNTs and CNFs have similar densities of about 2 g/cm^3 which results in about 1.44 g of CNT/CNF composite fabrics. The average CNT weights of 1, 3 and 5 wt.% is 0.0144, 0.0432, and 0.072 g, respectively. Single CNT weight is about 10^{-12} g which results in about 1×10^{10}, 4×10^{10}, and 7×10^{10} number of CNTs for 1, 3, and 5 wt.% CNTs, respectively.

The number of fully backed CNTs in NZ through 6-mm length is 10^{12} which gives backing density of 0.01, 0.04, and 0.07 % or in another word a volume fraction with Al substrate

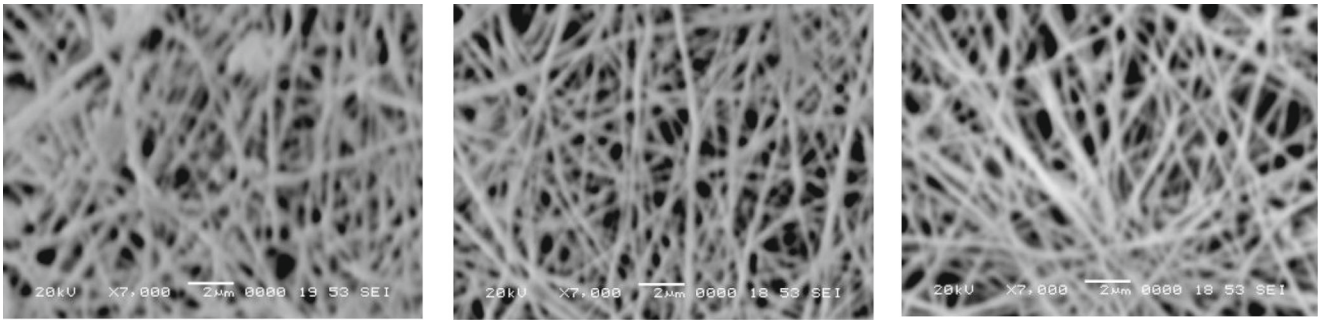

Fig. 2 Scanning electron microscope for CNT/CNF hybrid fabrics

of 0.01, 0.04, and 0.07 % for 1, 3, and 5 wt.% CNTs, respectively.

Based on previous calculations, the number of CNTs contributed in each NZ area is about 48×10^4, 19×10^5, and 33×10^5 for 1, 3, and 5 wt.% CNTs, respectively, assuming full CNTs alignment. The obvious difference in the numbers of CNTs for each weight% will have a noticeable effect on the mechanical properties of CNTs/CNFs/Al MMNCs especially for micro-hardness measurements.

Figure 5 represents the effect of the rotating and travelling directions of the tool; according to the dark area shown in Fig. 4, the tool rotates in counter clockwise direction and travels into the page forming narrow distribution at the retreating side (left), where the tool rotation is opposite to the tool travel direction (parallel to the direction of metal flow) and ending with wider distribution at the advancing side (right) where the tool rotation direction is the same as the tool travel direction (opposite the direction of metal flow). Also, the shown dark area represents the typical shape of the thermo-mechanically affected zone (TMAZ) [35], which also covers the distribution of CNT/CNF hybrid fabrics.

As a result of the tool action and influence on the substrates, when performed properly, a solid-state area is produced, that is, no melting. Because of various geometrical features on the tool, material movement around the pin can be complex, with gradients in strain, temperature, and strain rate. Accordingly, the resulting nugget zone (NZ) microstructure reflects these different thermo-mechanical histories and is not homogeneous. In spite of the local microstructural inhomogeneity, one of the significant benefits of this solid-state FSP is the fully recrystallized, equiaxed, fine-grain microstructure created in the NZ by the intense plastic deformation

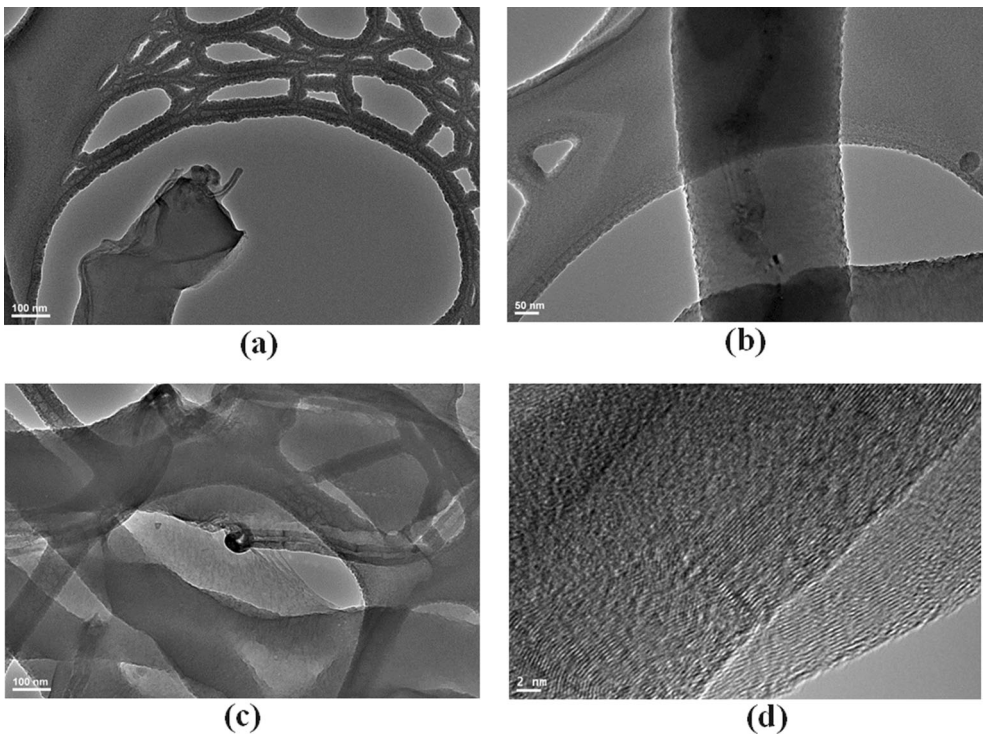

Fig. 3 HRTEM miroscope for 3 wt.% CNT/CNF hybrid fabrics. **a**, **b** Single CNT/CNF hybrid fabrics in different locations, **c** CNTs separated from carbon fibers, **d** CNT graphitic lamellas of 0.333-nm thickness

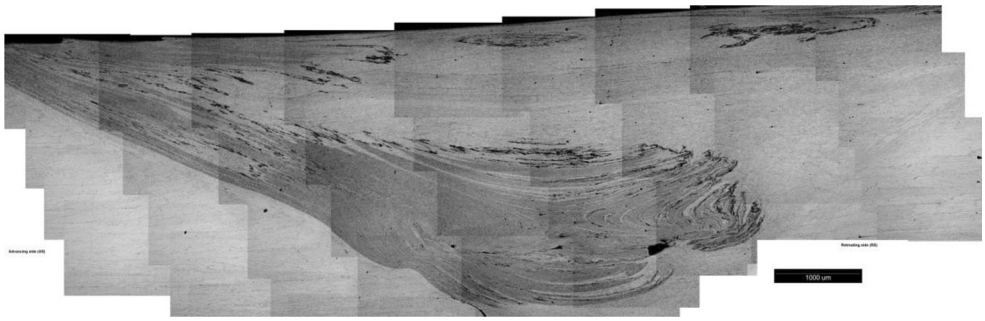

Fig. 4 SEM micrograph for CNTs/CNFs/Al MMNCs by FSP

at elevated temperature. As it has been reported in literatures [35], the fine-grain microstructure produces excellent mechanical properties, fatigue properties, enhanced formability, and exceptional super-plasticity.

3.2 Mechanical characterization

Tensile testing for 1, 3, and 5 wt.% CNT/CNF hybrid fabrics have been analyzed. Also, tensile and micro-hardness tests to the FSP MMNCs (CNT/CNF hybrid fabric-reinforced aluminum metal matrix) have been analyzed at all CNT reinforcement weight percent.

3.2.1 Tensile properties

Hot-pressed CNT/CNF hybrid fabrics have been tested and the result is shown in Fig. 5. The presence of CNTs in randomness electrospun pattern of CNFs reduces the strength of the hot-pressed fabrics from 54.5±3.5 to 44±2.7 to 34±7.5 MPa for 1, 3, and 5 CNT weight percent, respectively, as it might be attributed to the de-bonding effect of CNTs that has been attached at the surface of CNFs as it has been detected and presented in Fig. 3a; more explanation for such behavior has been demonstrated in Ali's and co-worker previous work [10, 17, 34].

Figure 6 presents the measurements of strength values for base metal (BM) aluminum matrix before and after FSP. The FSP has three parameters which affect aluminum matrix strength: the first is grain refinement which increases the strength, the second is the creation of low density of dislocation which decreases the strength, and the third is the coarsening and partial dissolution of precipitates as a result of increase in temperature which also decreases the strength. From the measurements, it is obvious that the grain refinement during FSP is dominated for aluminum metal matrix type of materials more than the other two parameters; consequently, BM strength increases from 78 to 105 MPa.

As shown in Fig. 7, the presence of CNT weight percent in nanofibril hybrid fabrics of strength less than stirred aluminum has soften the MMNCs, in general, as a rational effect for the presence of graphitic structure of CNFs in aluminum matrix (from 105 to 93 MPa). On the other hand, increases in strength for the MMNCs have been detected as CNT weight percent increases (from 91.7 for 1 wt.% to 95.2 for 3 wt.% to 97.3 MPa for 5 wt.% of CNTs) which conflicts, for the first look, with the previous fabric's strength values that can be explained due to the easily separation of CNTs from CNFs during FSP and accordingly CNTs with its huge numbers (48×10^4, 19×10^5, and 33×10^5 for 1, 3, and 5 wt.% CNTs, respectively) have worked separately, as proved in Fig. 3c, within the aluminum matrix and acted as a reinforcement element with its superior strength property which is not fully contributed previously in a beneficial way at the electrospun fabrics level. However, the low values of CNT volume fraction in Al substrates (0.01, 0.04, and 0.07 % for 1, 3, and 5 wt.% CNTs, respectively) could not play a sensible effect on BM strength values to strengthen the MMNCs due to the presence of CNFs that reduces the strength below the reported

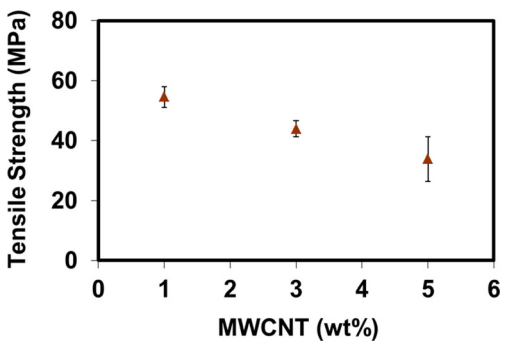

Fig. 5 Strength values of electrospun CNT/CNF composite fabrics

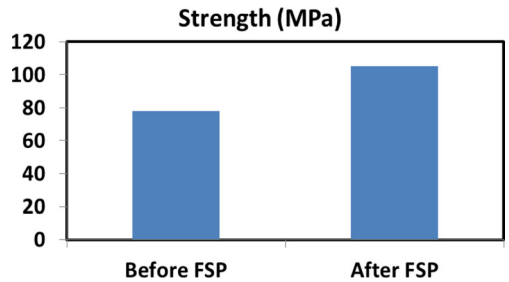

Fig. 6 Effect of FSP on (BM) aluminum matrix strength

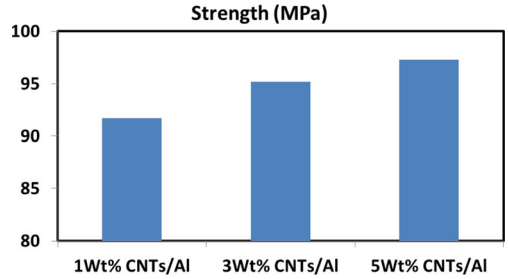

Fig. 7 Strength measurements of CNTs/CNFs/Al (MMNCs) by FSP

FSP BM values. However, micro-hardness measurements will reveal such speculation.

3.2.2 Hardness properties

The micro-hardness (more than one reading) along the centerline of the cross-section of the processed zone under the same stirring process conditions (2°, 1040 rpm, and 52 mm/min) has been measured and presented in Table 1. Also, the effect of zone and side type has been reported in Table 2. These results are correlated to the microstructure micrograph shown in Fig. 4. Four primary zones have been detected as follows:

1. The base metal (BM) or unaffected material or parent metal: this is material remote from the FSP that has not been deformed and that, although it may have experienced a thermal cycle from the weld, is not affected by the heat in terms of micro-structure or mechanical properties. The average reported hardness value for pure aluminum, 1, 3, and 5 wt.% CNTs/CNFs/Al MMNCs are 36.4, 36.7, 37.9, and 38 HV, respectively.
2. The heat-affected zone (HAZ) in this region, which lies closer to the friction stir center: the material has experienced a thermal cycle that has modified the microstructure and/or the mechanical properties. However, there is no plastic deformation occurring in this area. The average reported hardness value for pure aluminum, 1, 3 and 5 wt.% CNTs/CNFs/Al MMNCs are 37.4, 38.2, 38.9, and 39 HV for advancing side and 37.1, 37.8, 38.8, and 38.9 for retreating side, respectively.
3. The thermo-mechanically affected zone (TMAZ) in this region: the FSP tool has plastically deformed the material, and the heat from the process will also have exerted some influence on the material. In the case of aluminum, it is possible to obtain significant plastic strain without recrystallization in this region, and there is generally a distinct boundary between the recrystallized zone (NZ) and the deformed zones of the TMAZ. The average reported hardness value for pure aluminum, 1, 3, and 5 wt.% CNTs/CNFs/Al MMNCs are 37.2, 39.8, 39.9, and 40.5 HV for advancing side and 36.4, 38.5, 38.6, and 39.7 for retreating side, respectively.
4. The stir zone (SZ) refers to the zone previously occupied by the tool pin. FSP causes intense plastic deformation resulting in significant microstructural refinement and fully recrystallized of the processed zone increasing the hardness value. The average reported hardness value for pure aluminum, 1, 3, and 5 wt.% CNTs/CNFs/Al MMNCs are 39.4, 40.8, 41.3, and 42.4 HV, respectively.

Table 1 Micro-hrdness measured values (HV) for BM and MMNCs after FSP

Distance from center (mm)		Micro-hardness measured values (HV)			
		BM	1 wt.% CNTs	3 wt.% CNTs	5 wt.% CNTs
Advancing side	10	35.5	36.6	37.4	37.5
	9	36.6	36.2	41.4	38.1
	8	37.1	37.4	39.2	38.5
	7	38.3	39	39.3	38.9
	6	37.9	37.6	38.7	39
	5	36.1	37.9	38.8	39.1
	4	35.8	36.9	37.4	39.2
	3	37.7	41.1	41.2	40.4
	2	38	41.4	41.2	41.9
	1	39.4	40.4	40.9	42.3
Center		40	41.8	42.2	43.6
Retreating side	−1	38.9	40.1	40.8	41.4
	−2	37.4	40.7	40.2	41.3
	−3	36	37.1	37.3	39.6
	−4	35.8	37.8	38.2	38.1
	−5	35.9	37.6	38.4	39.2
	−6	37.1	37.3	38.5	38.9
	−7	38.2	38.6	39.6	38.7
	−8	36.9	36.3	38.7	38.9
	−9	36.1	36.8	37.6	37.4
	−10	35.2	36.3	36.6	37.2

Tables 1 and 2 represent the measured hardness values for FSP pure aluminum, 1, 3, and 5 wt.% CNTs/CNFs/Al MMNCs. From Table 2, it can be noticed that hardness values have been presented and correlated to the four regions SZ, TMAZ, HAZ, and BM as well as tool rotating directions (advancing and retreating). The reported values prove a consistency with reported data in literature related to each zone values as well as with measured strength values.

As shown in Fig. 8 and represented in Table 2, the average hardness values of the SZ for pure Al, 1, 3, and 5 wt.% CNTs/CNFs/Al MMNCs are 39.4, 40.8, 41.3, and 42.4 HV, respectively. We believe that the improvement in the hardness of the SZ is related to the grain size refinement and presence of

Table 2 Average hardness values (HV) for FSP zones

Side/Zone type		Average micro-hardness measured values (HV)			
		BM	1 wt.% CNTs	3 wt.% CNTs	5 wt.% CNTs
Advancing side	BM	36.4	36.7	37.9	38.0
	HAZ	37.4	38.2	38.9	39.0
	TMAZ	37.2	39.8	39.9	40.5
	SZ	39.4	40.8	41.3	42.4
Retreating side	SZ	39.4	40.8	41.3	42.4
	TMAZ	36.4	38.5	38.6	39.7
	HAZ	37.1	37.8	38.8	38.9
	BM	36.1	36.5	37.6	37.8

CNTs. Firstly, the grains of the SZ were finer than those in the BM and it is well known that fine grains play an important role in strengthening a material. Secondly, the presence of well-dispersed CNT weight percent in aluminum metal matrix resulted in increasing the hardness due to dispersion strengthening mechanism as shown in Fig. 8 and Table 2, as CNT weight percent increases all measured average hardness values increase. Also, as represented in Table 2 the advancing side shows better hardness values than retreating side as it has been proved from MMNCs micrograph assembly shown in Fig. 4, there were much CNTs/CNFs hybrid fabrics in advancing side more than retreating side.

4 Conclusions

Electrospinning with hot-pressing technique has been used to produce CNT/CNF firm, flexible, and strong hybrid fabrics; then, FSP has been utilized with both fabrics of different CNT weight percent and aluminum substrate to produce MMNCs (CNTs/CNFs/Al).

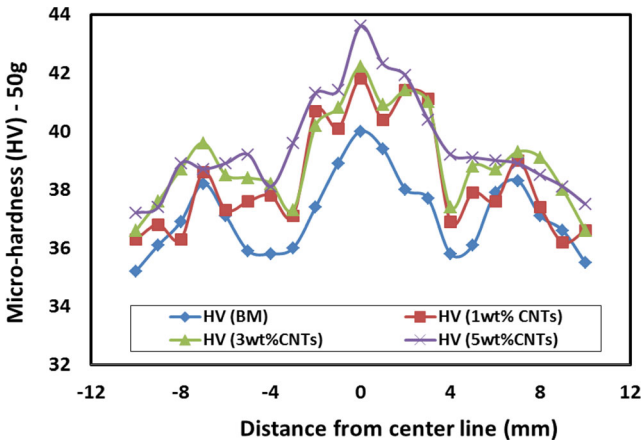

Fig. 8 Micro-hardness profiles of CNTs/CNFs/Al MMNCs by FSP

Conclusions can be stated in the following points:

1. A novel electrospinning and friction stir Bi-processing technique has been introduced for the first time to produce MMNCs (CNTs/CNFs/Al) of uniform and well-aligned reinforcements.
2. CNT/CNF hybrid fabrics by electrospinning technique have been produced at 1, 3, and 5 wt.% after hot pressing of electrospun fabrics.
3. The presence of CNTs in electrospun randomness pattern of CNFs reduces the strength of the hot-pressed CNT/CNF hybrid fabrics from 54.5±3.5 to 44±2.7 to 34±7.5 MPa for 1, 3, and 5 CNT weight percentage, respectively.
4. FSP increases aluminum BM strength from 78 to 105 MPa due to grain refinement mechanism domination.
5. CNT weight percent presented in electrospun nanofibril composite fabrics has a positive effect on the strength and hardness of MMNCs produced by FSP. However, CNFs soften the MMNCs and resulted in overall lower strength values.
6. Increase in strength from 91.7 to 95.2 to 97.3 MPa for the MMNCs has been detected as CNT weight percent increases from 1 to 3 to 5 wt.%, respectively.
7. Micro-hardness measurements of NZ including four primary zones: the base metal (BM), the heat-affected zone (HAZ), the thermo-mechanically affected zone (TMAZ), and the stir zone (SZ) has showed consistency with literature as well as strength measured values.
8. Hardness measured values in SZ increases from 39.4 to 40.8 to 41.3 to 42.4 HV for pure aluminum, 1, 3, and 5 wt.% CNTs/CNFs/Al MMNCs, respectively.
9. Advancing side reported higher hardness values than retreating side which has been correlated to the presence of more CNT/CNF hybrid fabrics as it has been proved from MMNC FSP micrograph.
10. Reported hardness values has increased from 38 to 39 to 40.5 to 42.4 for BM to HAZ to TMAZ to SZ on advancing side and from 37.8 to 38.9 to 39.7 to 42.4 on retreating side for 5 wt.% CNTs/CNFs/Al MMNCs.

Final remark CNT volume fraction with aluminum metal matrix is restricted due to its presence in preloaded fabric, and it was ranged between 0.01 and 0.07 %; these values should be increased by optimizing FSP for tool geometry, multiple passes, and groove shape and size.

Future work Tribological properties for the produced CNTs/CNFs/Al MMNCs are under investigations and will be measured in future work. CNTs along with CNFs expect to have good tribological behaviors as both have self-lubricant behavior. Especially, tribological properties of CNT/CNF hybrid fabrics showed an outstanding behavior in previous published work by Ali's et al. [34].

Acknowledgments The authors would like to thank Nano Technology Center (NTC), Mechanical Design and Production Engineering Department, Faculty of Engineering, Zagazig University, Egypt, for contributing in electrospinning and hot pressing as well as supplying nanofibril hybrid fabrics. Also, the authors would like to thank Tabbin Institute for Metallurgical Studies (TIMS), Helwan, Egypt, for allowing FSP and microhardness measurements.

References

1. Ali AA, El-Hamid MA (2006) Electro-spinning optimization for precursor carbon nano fibers. J Compos A 37:1681–1687
2. Rutledge GC, Fridrikh SV (2007) Formation of fibers by electrospinning. Adv Drug Deliv 59:1384–1391
3. Yordem OS, Papila M, Menceloglu YZ (2008) Effect of electrospinning parameters on polyacrylonitrile nanofibers diameter: an investigation by response surface methodology. Mater Des 29:34–44
4. Reneker DH, Yarin AL (2008) Electrospinning jets and polymer nanofibers. Polymer 49:2387–2425
5. Bhardwaj N, Kundu SC (2010) Electrospinning: a fascinating fiber fabrication technique. Biotechnol Advancements 28:325–347
6. Wang X, Ding B, Sun G, Wang M, Yu J (2013) Electro-spinning/netting: a strategy for the fabrication of three-dimensional polymer nano-fiber/nets. Prog Mater Sci 58:1173–1243
7. Ali AA (2008) New generation of super absorber nano fibroses hybrid fabric by electro-spinning. Mater Process Technol 199:193–198
8. Ko F, Gogotsi Y, Ali AA, Naguib N, Ye H, Yang G et al (2003) Electrospinning of continuous carbon nanotube-filled nanofiber yarns. Adv Mater 15:1161–1165
9. Mack J, Viculis L, Ali AA, Luoh R, Yang G, Hahn T et al (2005) Graphite nanoplatelet reinforcement of electrospun polyacrylonitrile nanofibers. Adv Mater 17:77–80
10. Ali AA, Rutledge GC (2009) Hot-pressed electrospun PAN nanofibers: an idea for flexible carbon mat. Mater Process Technol 209: 4617–4620
11. Dingreville R, Qu J, Cherkaoui M (2005) Surface free energy and its effect on the elastic behavior of nano-sized particles, wires and films. J Mech Phys Solids 53:1827–1854
12. Nanda KK, Maisels A, Kruis FE, Fissan H, Stappert S (2003) Highersurface energy of free nanoparticles. Phys Rev Lett 91(10): 106102, -1-4
13. Ji-H H, Wan Y-Q, Xu L (2007) Nano-effects, quantum-like properties in electrospun nanofibers. Chaos Solitons Fractals 33:26–37
14. Guillou CL, Brunet F, Irifune T, Ohfuji H, Rouzaud JN (2007) Nanodiamond nucleation below 2273 K at 15 GPa from carbons with different structural organizations. Carbon 45:636–648
15. Sun LT, Gong JL, Zhu ZY, Zhu DZ, Wang ZX, Zhang W et al (2005) Synthesis and characterization of diamond nanowires from carbon nanotubes. Diam Relat Mater 14:749–752
16. Ali AA, Al-Asmari KA (2012) Wet electrospun CuNP/carbon nanofibril composites: potential application for micro surface mounted components. J Appl Nanosci 2:55–61
17. Ali AA (2014) A novel 3-D graphite structure from thermally stabilized electrospun MWCNTs/PAN nanofibril composite fabrics. Int J Adv Manuf Technol 70:1731–1738
18. Devaraju A, Kumar A, Kotiveerachari B (2013) Influence of rotational speed and reinforcements on wear and mechanical properties of aluminum hybrid composites via friction stir processing. Mater Des 45:576–585
19. Gupta M, Mohamed FA, Lavernia EJ (1990) Solidification behaviour of Al–Li–SiCp MMCs processed using variable co-deposition of multi-phase materials. Mater Manuf Process 5(2):165–196
20. Mabhali LAB, Pityana SL, Sacks N (2010) Laser surface alloying of aluminum (AA1200) with Ni and SiC powders. Mater Manuf Process 25(12):1397–1403
21. Mishra RS, Ma ZY, Charit I (2003) Friction stir processing: a novel technique for fabrication of surface composites. Mater Sci Eng A 341:307–310
22. Ma ZY (2008) Friction stir processing technology: a review. Metall Mater Trans A 39:642–658
23. Asadi P, Besharati Givi MK, Faraji G (2010) Producing ultrafine-grained AZ91 from as cast AZ91 by FSP. Mater Manuf Process 25(11):1219–1226
24. Dehghani K, Mazinani M (2011) Forming nanocrystalline surface layers in copper using friction stir processing. Mater Manuf Process 26(07):922–925
25. Devaraju A, Kumar A (2011) Dry sliding wear and static immersion corrosion resistance of aluminum alloy 6061-T6/SiCp metal matrix composite prepared via friction stir processing. Int J Adv Res Mech Eng 1(2):62–68
26. Ma ZY, Sharma SR, Mishra RS (2006) Microstructural modification of as-cast Al–Si–Mg alloy by friction stir processing. Metall Mater Trans A 37:3233–3236
27. Sharma SR, Mishra RS (2008) Fatigue crack growth behavior of friction stir processed aluminum alloy. Scr Mater 59:395–398
28. Mishra RS, Z Y. M (2005) Friction stir welding and processing. Mater Sci Eng R 50:1–78
29. Choi D-H, Kim Y-I, Kim D-U, Jung S-B (2012) Effect of SiC particles on microstructure and mechanical property of friction stir processed AA6061-T4. Trans Nonferrous Metals Soc China 22:614–618
30. Mishra RS, Ma ZY, Charit I (2003) Friction stir processing: a novel technique for fabrication of surface composite. Mater Sci Eng A 341(1–2):307–310
31. Mishra RS, Mahoney MW, McFadden SX, Mara NA, Mukherjee AK (2000) High strain rate super plasticity in a friction stir processed 7075 Al alloy [J]. Scr Mater 42(2):163–168
32. Salehi M, Saadatmand M, Aghazadeh Mohandesi J (2012) Optimization of process parameters for producing AA6061/SiC nanocomposites by friction stir processing. Trans Nonferrous Metals Soc China 22:1055–1063
33. Mazaheri Y, Karimzadeh F, Enayati MH (2011) A novel technique for development of A356/Al2O3 surface nanocomposite by friction stir processing. J Mater Process Technol 211:1614–1619
34. Ali AA, Eldesouky RA, Zoalfakar HS (2014) Mechanical and tribological properties of hot-pressed electrospun MWCNTs/carbon nanofibril composite fabrics. Int J Adv Manuf Technol 74:983–993
35. Mishra RS, Mahoney MW (2007) Friction stir welding and processing, Copyright © 2007 ASM International®, DOI:10.1361/fswp editors, p 1–5.